PRAMANA
— journal of
physics

Vol. 60, No. 4
April 2003
pp. 697–709

Superdense matter

THOMAS SCHÄFER
Department of Physics and Astronomy, State University of New York, Stony Brook,
NY 11794-3800, USA
Riken-BNL Research Center, Brookhaven National Laboratory, Upton, NY 11973, USA

Abstract. We review recent work on the phase structure of QCD at very high baryon density. We introduce the phenomenon of color superconductivity and discuss the use of weak coupling methods. We study the phase structure as a function of the number of flavors and their masses. We also introduce effective theories that describe low energy excitations at high baryon density. Finally, we comment on the possibility of kaon condensation at very large baryon density.

Keywords. Quantum chromodynamics; dense matter.

PACS Nos 12.38.Aw; 12.38.Mh

1. Color superconductivity

In the interior of compact stars, matter is compressed to densities several times larger than the density of ordinary matter. Unlike the situation in relativistic heavy-ion collisions, these conditions are maintained for essentially infinite periods of time and the material is quite cold. At low density quarks are confined, chiral symmetry is broken, and baryonic matter is described in terms of neutrons and protons as well as their excitations. At very large density, on the other hand, we expect that baryonic matter is described more effectively in terms of quarks rather than hadrons. As we shall see, these quarks can form new condensates and the phase structure of dense quark matter is quite rich.

At very high density the natural degrees of freedom are quark excitations and holes in the vicinity of the Fermi surface. Since the Fermi momentum is large, asymptotic freedom implies that the interaction between quasiparticles is weak. In QCD, because of the presence of unscreened long range gauge forces, this is not quite true. Nevertheless, we believe that this fact does not essentially modify the argument. We know from the theory of superconductivity that the Fermi surface is unstable in the presence of even an arbitrarily weak attractive interaction. At very large density, the attraction is provided by one-gluon exchange between quarks in a color anti-symmetric $\bar{3}$ state. High density quark matter is therefore expected to behave as a color superconductor [1–4].

Color superconductivity is described by a pair condensate of the form

$$\phi = \langle \psi^T C \Gamma_{\rm D} \lambda_{\rm C} \tau_{\rm F} \psi \rangle . \tag{1}$$

Here, C is the charge conjugation matrix, and $\Gamma_{\rm D}, \lambda_{\rm C}, \tau_{\rm F}$ are Dirac, color, and flavor matrices. Except in the case of only two colors, the order parameter cannot be a color singlet. Color superconductivity is therefore characterized by the breakdown of color gauge invariance. As usual, this statement has to be interpreted with care because local gauge invariance cannot really be broken. Nevertheless, we can study gauge invariant consequences of a quark pair condensate, in particular the formation of a gap in the excitation spectrum.

In addition to that, color superconductivity can lead to the breakdown of global symmetries. We shall see that in some cases there is a gauge invariant order parameter for the $U(1)$ of baryon number. This corresponds to true superfluidity and the appearance of a massless phonon. We shall also find that for $N_f > 2$ color superconductivity leads to chiral symmetry breaking. Finally, if the effects of finite quark masses are taken into account we find additional forms of long-range order.

2. Phase structure in weak coupling

2.1 *QCD with two flavors*

In this section we shall discuss how to use weak coupling methods in order to explore the phases of dense quark matter. We begin with what is usually considered to be the simplest case, quark matter with two degenerate flavors, up and down. Renormalization group arguments suggest [5,6], and explicit calculations show [7,8], that whenever possible quark pairs condense in an *s*-wave. This means that the spin wave function of the pair is anti-symmetric. Since the color wave function is also anti-symmetric, the Pauli principle requires the flavor wave function to be anti-symmetric too. This essentially determines the structure of the order parameter [9,10]

$$\phi^a = \langle \varepsilon^{abc} \psi^b C\gamma_5 \tau_2 \psi^c \rangle. \tag{2}$$

This order parameter breaks the color $SU(3) \to SU(2)$ and leads to a gap for up and down quarks with two out of the three colors. Chiral and isospin symmetry remain unbroken.

We can calculate the magnitude of the gap and the condensation energy using weak coupling methods. In weak coupling the gap is determined by ladder diagrams with the one gluon exchange interaction. These diagrams can be summed using the gap equation [11–15]

$$\Delta(p_0) = \frac{g^2}{12\pi^2} \int {\rm d}q_0 \int {\rm d}\cos\theta \times \left(\frac{\frac{3}{2} - \frac{1}{2}\cos\theta}{1 - \cos\theta + G/(2\mu^2)} + \frac{\frac{1}{2} + \frac{1}{2}\cos\theta}{1 - \cos\theta + F/(2\mu^2)} \right) \frac{\Delta(q_0)}{\sqrt{q_0^2 + \Delta(q_0)^2}}. \tag{3}$$

Here, $\Delta(p_0)$ is the frequency dependent gap, g is the QCD coupling constant and G and F are the self-energies of magnetic and electric gluons. This gap equation is very similar to the BCS gap equations that describe nuclear superfluids. The main difference is that because the gluon is massless, the gap equation contains a collinear $\cos\theta \sim 1$ divergence. In a dense medium the collinear divergence is regularized by the gluon self-energy. For $\vec{q} \to 0$ and to leading order in perturbation theory we have

$$F = 2m^2, \quad G = \frac{\pi}{2} m^2 \frac{q_0}{|\vec{q}|}, \tag{4}$$

with $m^2 = N_f g^2 \mu^2/(4\pi^2)$. In the electric part, $m_D^2 = 2m^2$ is the familiar Debye screening mass. In the magnetic part, there is no screening of static modes, but non-static modes are modes dynamically screened due to Landau damping.

We can now perform the angular integral and find

$$\Delta(p_0) = \frac{g^2}{18\pi^2} \int \mathrm{d}q_0 \log\left(\frac{b\mu}{|p_0 - q_0|}\right) \frac{\Delta(q_0)}{\sqrt{q_0^2 + \Delta(q_0)^2}}, \tag{5}$$

with $b = 256\pi^4 (2/N_f)^{5/2} g^{-5}$. We can now see why it was important to keep the frequency dependence of the gap. Because the collinear divergence is regulated by dynamic screening, the gap equation depends on p_0 even if the frequency is small. We can also see that the gap scales as $\exp(-c/g)$. The collinear divergence leads to a gap equation with a double-log behavior. Qualitatively

$$1 \sim \frac{g^2}{18\pi^2} \left[\log\left(\frac{\mu}{\Delta}\right)\right]^2, \tag{6}$$

from which we conclude that $\Delta \sim \exp(-c/g)$. The approximation (6) is not sufficiently accurate to determine the correct value of the constant c. A more detailed analysis shows that the gap on the Fermi surface is given by

$$\Delta_0 \simeq 512\pi^4 (2/N_f)^{5/2} \mu g^{-5} \exp\left(-\frac{3\pi^2}{\sqrt{2}g}\right). \tag{7}$$

We should emphasize that, strictly speaking, this result contains only an estimate of the pre-exponent. It was recently argued that wave function renormalization and quasiparticle damping give $O(1)$ contributions to the pre-exponent which substantially reduce the gap [15,16].

For chemical potentials $\mu < 1$ GeV, the coupling constant is not small and the applicability of perturbation theory is in doubt. If we ignore this problem and extrapolate the perturbative calculation to densities $\rho \simeq 5\rho_0$, we find gaps $\Delta \simeq 100$ MeV. This result may indeed be more reliable than the calculation on which it is based. In particular, we note that similar results have been obtained using realistic interactions which reproduce the chiral condensate at zero baryon density [9,10].

2.2 *QCD with three flavors: Color-flavor-locking*

If quark matter is formed at densities several times nuclear matter density we expect the quark chemical potential to be larger than the strange quark mass. We therefore have to determine the structure of the superfluid order parameter for three quark flavors. We begin with the idealized situation of three degenerate flavors. From the arguments given in the last section we expect the order parameter to be color and flavor anti-symmetric matrix of the form

$$\phi_{ij}^{ab} = \langle \psi_i^a C\gamma_5 \psi_j^b \rangle. \tag{8}$$

In order to determine the precise structure of this matrix we have to extremize grand canonical potential. We find [17,18]

$$\Delta_{ij}^{ab} = \Delta(\delta_i^a \delta_j^b - \delta_i^b \delta_j^a), \tag{9}$$

which describes the color-flavor locked phase proposed in [19]. Both color and flavor symmetries are completely broken. There are eight combinations of color and flavor symmetries that generate unbroken global symmetries. The symmetry breaking pattern is

$$SU(3)_L \times SU(3)_R \times U(1)_V \to SU(3)_V. \tag{10}$$

This is exactly the same symmetry breaking that QCD exhibits at low density. The spectrum of excitations in the color-flavor-locked (CFL) phase also looks remarkably like the spectrum of QCD at low density [20]. The excitations can be classified according to their quantum numbers under the unbroken $SU(3)$, and by their electric charge. The modified charge operator that generates a true symmetry of the CFL phase is given by a linear combination of the original charge operator $Q_{\rm em}$ and the color hypercharge operator $Q = \mathrm{diag}(-2/3, -2/3, 1/3)$. Also, baryon number is only broken modulo 2/3, which means that one can still distinguish baryons from mesons. We find that the CFL phase contains an octet of Goldstone bosons associated with chiral symmetry breaking, an octet of vector mesons, an octet and a singlet of baryons, and a singlet Goldstone boson related to superfluidity. All of these states have integer charges.

With the exception of the $U(1)$ Goldstone boson, these states exactly match the quantum numbers of the lowest lying multiplets in QCD at low density. In addition to that, the presence of the $U(1)$ Goldstone boson can also be understood. The $U(1)$ order parameter is $\langle (uds)(uds) \rangle$. This order parameter has the quantum numbers of a 0^+ $\Lambda\Lambda$ pair condensate. In $N_f = 3$ QCD, this is the most symmetric two-nucleon channel, and a very likely candidate for superfluidity in nuclear matter at low to moderate density. We conclude that in QCD with three degenerate light flavors, there is no fundamental difference between the high and low density phases. This implies that a low density hyper-nuclear phase and the high density quark phase might be continuously connected, without an intervening phase transition.

2.3 *Other phases*

Color-flavor locking can be generalized to QCD with more than three flavors [17]. Chiral symmetry is broken for all $N_f \geq 3$, but only in the case $N_f = 3$ do we find the $T = \mu = 0$ pattern of chiral symmetry breaking, $SU(N_f)_L \times SU(N_f)_R \to SU(N_f)_V$.

The case $N_f = 1$ is special [8]. In this case the order parameter is flavor-symmetric and the Cooper pairs carry non-zero angular momentum. For $N_c = 3$ the spin direction can become aligned with the color orientation of the Cooper pair. In the color-spin locked phase color and rotational invariance are broken, but a diagonal $SO(3)$ survives.

If the number of colors is very large, $N_c \to \infty$, color superconductivity is suppressed and the ground state is very likely a chiral density wave [21]. This state is analogous to spin density waves in condensed matter physics. If the baryon density is large, the transition from color superconductivity to chiral density waves requires very large values of N_c of the order of $N_c > 1000$ [22].

3. The role of the strange quark mass

At baryon densities relevant to astrophysical objects distortions of the pure CFL state due to non-zero quark masses cannot be neglected [23–28]. This problem can be studied using the effective chiral theory of the CFL phase [29] (CFLχTh). This theory determines both the ground state and the spectrum of excitations with energies below the gap in the CFL phase. Using the effective theory allows us to perform systematic calculations order by order in the quark mass.

3.1 *CFL chiral theory (CFLχTh)*

For excitation energies smaller than the gap the only relevant degrees of freedom are the Goldstone modes associated with the breaking of chiral symmetry and baryon number. The interaction of the Goldstone modes is described by an effective Lagrangian of the form [29]

$$\begin{aligned}\mathscr{L}_{\rm eff} = \frac{f_\pi^2}{4}{\rm Tr}\left[\nabla_0\Sigma\nabla_0\Sigma^\dagger - v_\pi^2\partial_i\Sigma\partial_i\Sigma^\dagger\right] + \left[C{\rm Tr}(M\Sigma^\dagger) + {\rm h.c.}\right]\\ +\left[A_1{\rm Tr}(M\Sigma^\dagger){\rm Tr}(M\Sigma^\dagger) + A_2{\rm Tr}(M\Sigma^\dagger M\Sigma^\dagger)\right.\\ \left.+A_3{\rm Tr}(M\Sigma^\dagger){\rm Tr}(M^\dagger\Sigma) + {\rm h.c.}\right] + \cdots.\end{aligned} \tag{11}$$

Here $\Sigma = \exp(i\phi^a\lambda^a/f_\pi)$ is the chiral field, f_π is the pion decay constant and M is a complex mass matrix. The chiral field and the mass matrix transform as $\Sigma \to L\Sigma R^\dagger$ and $M \to LMR^\dagger$ under chiral transformations $(L,R) \in SU(3)_L \times SU(3)_R$. We have suppressed the singlet fields associated with the breaking of the exact $U(1)_V$ and approximate $U(1)_A$ symmetries. The theory (11) looks superficially like ordinary chiral perturbation theory. There are, however, some important differences. Lorentz invariance is broken and Goldstone modes move with the velocity $v_\pi < c$. The chiral expansion has the structure

$$\mathscr{L} \sim f_\pi^2\Delta^2\left(\frac{\partial_0}{\Delta}\right)^k\left(\frac{\vec{\partial}}{\Delta}\right)^l(\Sigma)^m(\Sigma^\dagger)^n. \tag{12}$$

Loop graphs are suppressed by powers of $\partial/(4\pi f_\pi)$. We shall see that the pion decay constant scales as $f_\pi \sim p_{\rm F}$. As a result higher order derivative interactions are parametrically more important than loop diagrams with the leading order vertices.

Further differences as compared to chiral perturbation theory in vacuum appear when the expansion in the quark mass is considered. The CFL phase has an approximate $(Z_2)_A$ symmetry under which $M \to -M$ and $\Sigma \to \Sigma$. This symmetry implies that the coefficients of mass terms that contain odd powers of M are small. The $(Z_2)_A$ symmetry is explicitly broken by instantons. The coefficient C can be determined from a weak coupling instanton calculation and $C \sim (\Lambda_{\rm QCD}/p_{\rm F})^8$ [17,30]. BCS calculations show that the CFL phase undergoes a phase transition to a less symmetric phase when $m^2/(2p_{\rm F}) \sim \Delta$ [23,24]. This suggests that the expansion parameter in the chiral expansion is $M^2/(p_{\rm F}\Delta)$. We shall see that this is indeed the case. However, the coefficients A_i of the quadratic terms in M turn out to be anomalously small

$$A_i M^2 \sim \Delta^2 M^2 \sim f_\pi^2 \Delta^2 \left(\frac{M^2}{p_{\rm F}^2}\right), \tag{13}$$

compared to the naive estimate $A_i M^2 \sim f_\pi^2 \Delta^2 [M^2/(p_{\rm F}\Delta)]$.

The pion decay constant f_π and the coefficients A_i can be determined using matching techniques. Matching expresses the requirement that Green functions in the effective chiral theory and the underlying microscopic theory, QCD, agree. The pion decay constant is most easily determined by coupling $SU(N_f)_{L,R}$ gauge fields $W_{L,R}$ to the left and right flavor currents. As usual, this amounts to replacing ordinary derivatives by covariant derivatives. The time component of the covariant derivative is given by $\nabla_0 \Sigma = \partial_0 \Sigma + i W_L \Sigma - i \Sigma W_R$, where we have suppressed the vector index of the gauge fields. In the CFL vacuum $\Sigma = 1$ the axial gauge field $W_L - W_R$ acquires a mass by the Higgs mechanism. From (11) we get

$$\mathscr{L} = \frac{f_\pi^2}{4} \frac{1}{2} (W_L - W_R)^2. \tag{14}$$

The coefficients $A_{1,2,3}$ can be determined by computing the shift in the vacuum energy due to non-zero quark masses in both the chiral theory and the microscopic theory. In the chiral theory we have

$$\Delta\mathscr{E} = -[A_1 \left({\rm Tr}(M)\right)^2 + A_2 {\rm Tr}(M^2) + A_3 {\rm Tr}(M) {\rm Tr}(M^\dagger) + {\rm h.c.}]. \tag{15}$$

We note that different $O(M^2)$ mass terms produce distinct contributions to the vacuum energy. This means that the coefficients A_i can be reconstructed uniquely from the vacuum energy.

3.2 *High density effective theory (HDET)*

In this section we shall determine the mass of the gauge field and the shift in the vacuum energy in the CFL phase of QCD at large baryon density. This is possible because asymptotic freedom guarantees that the effective coupling is weak. The QCD Lagrangian in the presence of a chemical potential is given by

$$\mathscr{L} = \bar\psi \left(i \not{D} + \mu \gamma_0\right) \psi - \bar\psi_L M \psi_R - \bar\psi_R M^\dagger \psi_L - \frac{1}{4} G^a_{\mu\nu} G^a_{\mu\nu}, \tag{16}$$

where $D_\mu = \partial_\mu + igA_\mu$ is the covariant derivative, M is the mass matrix and μ is the baryon chemical potential. If the baryon density is very large, perturbative QCD calculations can be further simplified. The main observation is that the relevant degrees of freedom are particle and hole excitations in the vicinity of the Fermi surface. We shall describe these excitations in terms of the field $\psi_+(\vec{v}_{\rm F}, x)$, where $\vec{v}_{\rm F}$ is the Fermi velocity. At tree level, the quark field ψ can be decomposed as $\psi = \psi_+ + \psi_-$, where $\psi_\pm = \frac{1}{2}(1 \pm \vec{\alpha} \cdot \hat{v}_{\rm F})\psi$. To leading order in $1/p_{\rm F}$ we can eliminate the field ψ_- using its equation of motion. For $\psi_{-,L}$ we find

$$\psi_{-,L} = \frac{1}{2p_{\rm F}} (i \vec{\alpha}_\perp \cdot \vec{D} \psi_{+,L} + \gamma_0 M \psi_{+,R}). \tag{17}$$

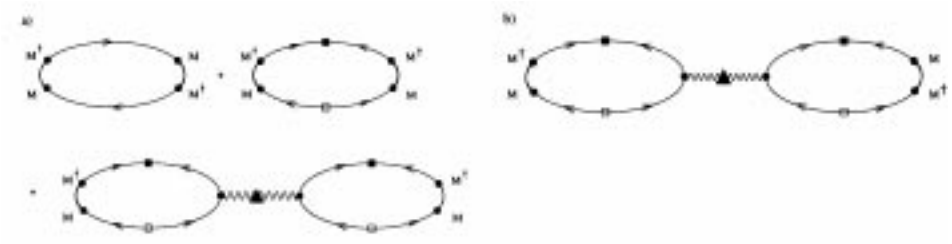

Figure 1. This figure shows the contribution to the vacuum energy from the effective chemical potential terms in the high density effective theory. Figure (**a**) shows the diagrams that are matched against the $(MM^\dagger)^2$ term and (**b**) shows the diagram that is matched against the $MM^\dagger\Sigma M^\dagger M\Sigma$ term in the chiral theory.

There is a similar equation for $\psi_{-,R}$. The longitudinal and transverse components of γ_μ are defined by $(\gamma_0,\vec{\gamma})_\parallel = (\gamma_0,\vec{v}(\vec{\gamma}\cdot\vec{v}))$ and $(\gamma_\mu)_\perp = \gamma_\mu - (\gamma_\mu)_\parallel$. To leading order in $1/p_{\rm F}$ the Lagrangian for the ψ_+ field is given by [31–33]

$$\begin{aligned}\mathscr{L} = {} & \psi^\dagger_{L+}(iv\cdot D)\psi_{L+} - \frac{\Delta}{2}(\psi^{ai}_{L+}C\psi^{bj}_{L+}(\delta_{ai}\delta_{bj}-\delta_{aj}\delta_{bi}) + \text{h.c.}) \\ & -\frac{1}{2p_{\rm F}}\psi^\dagger_{L+}\left((\not{D}_\perp)^2 + MM^\dagger\right)\psi_{L+} + \left(R\leftrightarrow L, M\leftrightarrow M^\dagger\right) + \cdots, \end{aligned} \tag{18}$$

with $v_\mu = (1,\vec{v})$ and $i,j,\ldots$ and $a,b,\ldots$ denote flavor and color indices. In order to perform perturbative calculations in the superconducting phase we have added a tree level gap term $\psi^{ai}_{L,R}C\Delta_{ai,bj}\psi^{bj}_{L,R}$. In the CFL phase this term has the structure $\Delta_{ai,bj} = \Delta(\delta_{ai}\delta_{bj}-\delta_{aj}\delta_{bi})$. The magnitude of the gap Δ is determined order by order in perturbation theory from the requirement that the thermodynamic potential is stationary with respect to Δ. With the gap term included the perturbative expansion is well-defined. There are no additional infra-red divergences. In particular, there is no need to include additional gap parameters at higher order in $1/p_{\rm F}$, such as the anti-particle gap or modifications of the particle gap due to non-zero quark masses [34].

The screening mass of the flavor gauge fields $W_{L,R}$ can be determined by computing the corresponding polarization function in the limit $q_0 = 0$, $\vec{q}\to 0$. We find $\Pi^{LL}_{00} = \Pi^{RR}_{00} = -\Pi^{LR}_{00} = m_D^2/4$ with $m_D^2 = (21-8\log(2))p_{\rm F}^2/(36\pi^2)$. Matching this result against eq. (14), we get [35]

$$f_\pi^2 = \frac{21-8\log(2)}{18}\left(\frac{p_{\rm F}^2}{2\pi^2}\right). \tag{19}$$

Our next task is to compute the mass dependence of the vacuum energy. To leading order in $1/p_{\rm F}$ there is only one operator in the high density effective theory

$$\mathscr{L} = -\frac{1}{2p_{\rm F}}\left(\psi^\dagger_{L+}MM^\dagger\psi_{L+} + \psi^\dagger_{R+}M^\dagger M\psi_{R+}\right). \tag{20}$$

This term arises from expanding the kinetic energy of a massive fermion around $p = p_{\rm F}$. We note that $MM^\dagger/(2p_{\rm F})$ and $M^\dagger M/(2p_{\rm F})$ act as effective chemical potentials for left

and right-handed fermions, respectively. Indeed, to leading order in the $1/p_{\rm F}$ expansion, the Lagrangian (18) is invariant under a time dependent flavor symmetry $\psi_L \to L(t)\psi_L$, $\psi_R \to R(t)\psi_R$ where $X_L = MM^\dagger/(2p_{\rm F})$ and $X_R = M^\dagger M/(2p_{\rm F})$ transform as left- and right-handed flavor gauge fields. If we impose this approximate gauge symmetry on the CFL chiral theory we have to include the effective chemical potentials $X_{L,R}$ in the covariant derivative of the chiral field [27],

$$\nabla_0\Sigma = \partial_0\Sigma + i\left(\frac{MM^\dagger}{2p_{\rm F}}\right)\Sigma - i\Sigma\left(\frac{M^\dagger M}{2p_{\rm F}}\right). \tag{21}$$

X_L and X_R contribute to the vacuum energy at $O(M^4)$,

$$\Delta\mathscr{E} = \frac{f_\pi^2}{8p_{\rm F}^2}{\rm Tr}\left[(MM^\dagger)(M^\dagger M) - (MM^\dagger)^2\right]. \tag{22}$$

This result can also be derived directly in the microscopic theory [27]. The corresponding diagrams are shown in figure 1. We also note that eq. (22) has the expected scaling behavior $\mathscr{E} \sim f_\pi^2\Delta^2[M^2/(p_{\rm F}\Delta)]^2$.

$O(M^2)$ terms in the vacuum energy are generated by terms in the high density effective theory that are higher order in the $1/p_{\rm F}$ expansion. We recently argued that these terms can be determined by computing chirality violating quark–quark scattering amplitudes for fermions in the vicinity of the Fermi surface [34]. Feynman diagrams for $q_L + q_L \to q_R + q_R$ are shown in figure 2a. To leading order in the $1/p_{\rm F}$ expansion the chirality violating scattering amplitudes are independent of the scattering angle and can be represented as local four-fermion operators

$$\mathscr{L} = \frac{g^2}{8p_{\rm F}^4}((\psi_L^{A\dagger}C\psi_L^{B\dagger})(\psi_R^C C\psi_R^D)\Gamma^{ABCD} + (\psi_L^{A\dagger}\psi_L^B)(\psi_R^{C\dagger}\psi_R^D)\tilde{\Gamma}^{ACBD}). \tag{23}$$

There are two additional terms with $(L \leftrightarrow R)$ and $(M \leftrightarrow M^\dagger)$. We have introduced the CFL eigenstates ψ^A defined by $\psi_i^a = \psi^A(\lambda^A)_{ai}/\sqrt{2}$, $A = 0,\ldots,8$. The tensors Γ is defined by

$$\Gamma^{ABCD} = \frac{1}{8}\Big\{{\rm Tr}\left[\lambda^A M(\lambda^D)^T\lambda^B M(\lambda^C)^T\right] - \frac{1}{3}{\rm Tr}[\lambda^A M(\lambda^D)^T]{\rm Tr}[\lambda^B M(\lambda^C)^T]\Big\}. \tag{24}$$

The second tensor $\tilde{\Gamma}$ involves both M and $M^\dagger$ and only contributes to terms of the form ${\rm Tr}[MM^\dagger]$ in the vacuum energy. These terms do not contain the chiral field Σ and therefore do not contribute to the masses of Goldstone modes. We can now compute the shift in the vacuum energy due to the effective vertex (23). The leading contribution comes from the two-loop diagram shown in figure 2b. We find

$$\Delta\mathscr{E} = -\frac{3\Delta^2}{4\pi^2}\{({\rm Tr}[M])^2 - {\rm Tr}[M^2]\} + (M \leftrightarrow M^\dagger). \tag{25}$$

Using this result we can determine the coefficients $A_{1,2,3}$ in the CFL chiral theory. We obtain

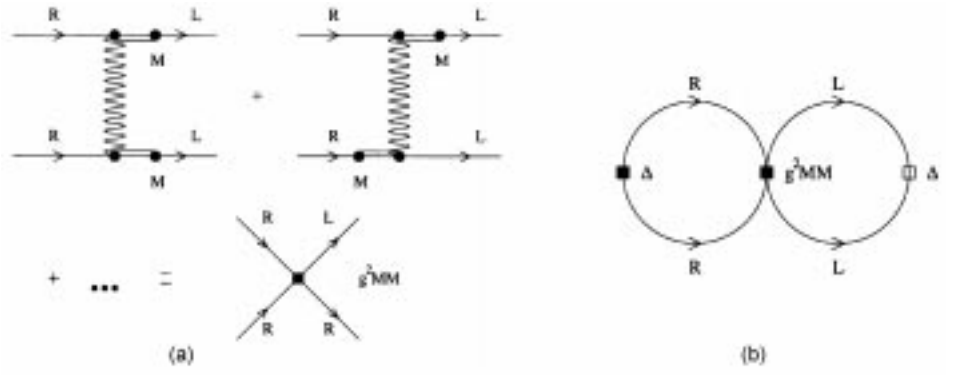

(a) (b)

Figure 2. Figure (**a**) shows the effective chirality violating four-fermion vertex in the high density effective theory. Figure (**b**) shows the corresponding contribution to the vacuum energy. As explained in the text, there are additional vertices which involve $MM^\dagger$, but they do not contribute to the masses of Goldstone modes.

$$A_1 = -A_2 = \frac{3\Delta^2}{4\pi^2}, \quad A_3 = 0, \tag{26}$$

which agrees with the result of Son and Stephanov [35]. We also note that $\mathscr{E} \sim f_\pi^2 \Delta^2 (\Delta/p_{\rm F})$ $[M^2/(p_{\rm F}\Delta)]$ which shows that the coefficients A_i are suppressed by $(\Delta/p_{\rm F})$. The effective Lagrangian (18) and (23) can also be used to compute higher order terms in M. The dominant $O(M^4)$ term is the effective chemical potential term eq. (22). Other $O(M^4)$ terms are suppressed by additional powers of $(\Delta/p_{\rm F})$.

3.3 *Kaon condensation*

Using the results discussed in the previous section we can compute the masses of Goldstone bosons in the CFL phase. In §3.1 we argued that the expansion parameter in the chiral expansion of the Goldstone boson masses is $\delta = m^2/(p_{\rm F}\Delta)$. The first term in this expansion comes from the $O(M^2)$ term in (11), but the coefficients A contain the additional small parameter $\varepsilon = (\Delta/p_{\rm F})$. In a combined expansion in δ and ε the $O(\varepsilon\delta)$ mass term and the $O(\delta^2)$ chemical potential term appear in the same order. At this order, the masses of the flavored Goldstone bosons are

$$\begin{aligned}
m_{\pi^\pm} &= \mp\frac{m_d^2 - m_u^2}{2p_{\rm F}} + \left[\frac{4A}{f_\pi^2}(m_u + m_d)m_s\right]^{1/2}, \\
m_{K_\pm} &= \mp\frac{m_s^2 - m_u^2}{2p_{\rm F}} + \left[\frac{4A}{f_\pi^2}m_d(m_u + m_s)\right]^{1/2}, \\
m_{K^0,\bar{K}^0} &= \mp\frac{m_s^2 - m_d^2}{2p_{\rm F}} + \left[\frac{4A}{f_\pi^2}m_u(m_d + m_s)\right]^{1/2}.
\end{aligned} \tag{27}$$

We observe that the pion masses are not strongly affected by the effective chemical potential but the masses of the K^+ and K^0 are substantially lowered while the K^- and $\bar{K}^0$ are pushed up. As a result the K^+ and K^0 meson become massless if $m_s \sim m_{u,d}^{1/3}\Delta^{2/3}$. For larger values of m_s the kaon modes are unstable, signaling the formation of a kaon condensate.

Once kaon condensation occurs the ground state is reorganized. For simplicity, we consider the case of exact isospin symmetry $m_u = m_d \equiv m$. Kaon condensation can be studied using an ansatz of the form $\Sigma = \exp(i\alpha\lambda_4)$. The vacuum energy is

$$V(\alpha) = -f_\pi^2\left(\frac{1}{2}\left(\frac{m_s^2-m^2}{2p_{\rm F}}\right)^2\sin(\alpha)^2 + (m_K^0)^2(\cos(\alpha)-1)\right), \tag{28}$$

where $(m_K^0)^2 = (4A/f_\pi^2)m_{u,d}(m_{u,d}+m_s)$ is the $O(M^2)$ kaon mass in the limit of exact isospin symmetry. Minimizing the vacuum energy we obtain $\alpha = 0$ if $m_s^2/(2p_{\rm F}) < m_K^0$ and $\cos(\alpha) = (m_K^0)^2/\mu_s^2$ with $\mu_s = m_s^2/(2p_{\rm F})$ if $\mu_s > m_K^0$. We observe that the vacuum energy is independent of θ_1, θ_2, ϕ. The hypercharge density is given by

$$n_Y = f_\pi^2\mu_s\left(1-\frac{(m_K^0)^4}{\mu_s^4}\right). \tag{29}$$

We observe that within the range of validity of the effective theory, $\mu_s < \Delta$, the hypercharge density satisfies $n_Y < \Delta p_{\rm F}^2/(2\pi^2)$. This means that the number of condensed kaons is bounded by the number of particles contained within a strip of width Δ around the Fermi surface. It also implies that near the unlocking transition, $\mu_s \sim \Delta$, the CFL state is significantly modified. In this regime, of course, we can no longer rely on the effective theory and a more microscopic calculation is necessary.

Let us summarize what we have learned about the effects of a non-zero strange quark mass m_s. The effect of m_s is controlled by the parameter $m_s^2/(p_{\rm F}\Delta)$. If $m_s^2/(p_{\rm F}\Delta) \sim 1$, color-flavor-locking breaks down and a transition to a less symmetric phase will occur. In the regime $m_s^2/(p_{\rm F}\Delta) < 1$ the phase structure can be established using the effective chiral theory of the CFL phase and dimensional analysis. We have argued that there is a new small scale $m_s^2/(p_{\rm F}\Delta) \sim (\sqrt{m_{u,d}m_s}/p_{\rm F}) \ll 1$ which corresponds to the onset of kaon condensation. If perturbative QCD is reliable we can be more quantitative. To leading order in g, the critical strange quark mass for kaon condensation is

$$m_s|_{\rm crit} = 3.03\cdot m_d^{1/3}\Delta^{2/3}. \tag{30}$$

This result suggests that for values of the strange quark mass and the gap that are relevant to compact stars CFL matter is likely to support a kaon condensate.

4. Conclusion: The many phases of QCD

We would like to conclude by summarizing some of the things we have learned about the phase structure of QCD-like theories at finite temperature and chemical potential. We begin with the case of two massless flavors, figure 3a. If we move along the chemical potential axis at temperature $T = 0$, there is a minimum chemical potential required in order to introduce baryons into the system. Since nuclear matter is self-bound, this point is a first

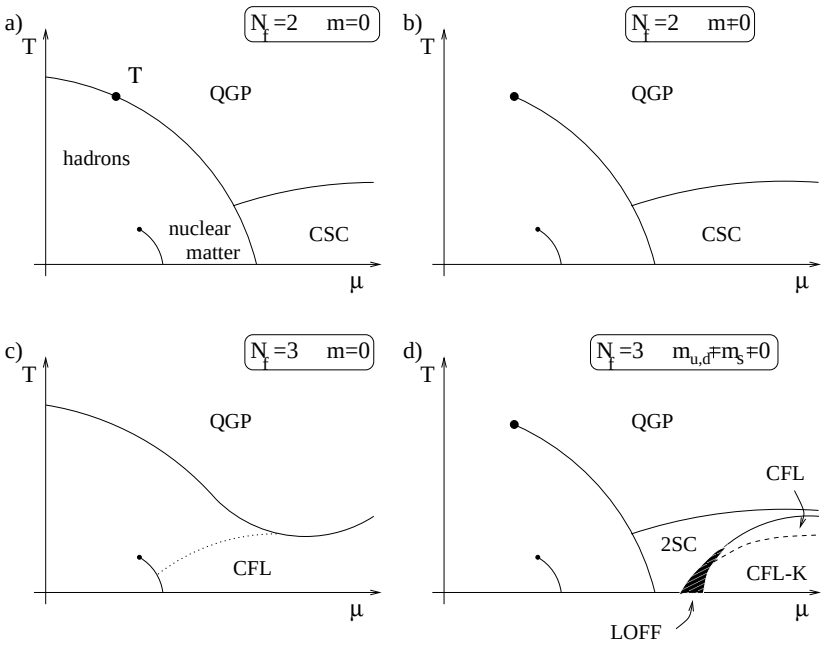

Figure 3. Schematic phase diagram of QCD at finite temperature and density. Figures (**a**)–(**d**) correspond to different numbers of massless and massive flavors, see the discussion in the text.

order transition. Along the temperature axis, the line of first order transitions eventually ends in a critical point: This is the endpoint of the nuclear liquid–gas phase transition. If we continue to increase the chemical potential, we encounter the various phases of nuclear matter at high density. Many possibilities have been discussed in the literature, and we have nothing to add to this discussion. At even higher chemical potential, we encounter the transition to quark matter and the two flavor quark superconductor. Model calculations suggest that this transition is first order. In the case of two massless flavors, universality arguments suggest, and lattice calculations support the idea that the finite temperature zero chemical potential chiral phase transition is second order. In this case, the line of first order $\mu \neq 0$ transitions would have to meet the $T \neq 0$ transition at a tricritical point [36,37].

This tricritical point is quite remarkable, because it remains a true critical point, even if the quark masses are not zero (figure 3b). A non-zero quark mass turns the second order $T \neq 0$ transition into a smooth crossover, but the first order $\mu \neq 0$ transition persists. While it is hard to predict where exactly the tricritical point is located in the phase diagram it may well be possible to settle the question experimentally. Heavy ion collisions at relativistic energies produce matter under the right conditions and experimental signatures of the tricritical point have been suggested [38].

We have already discussed the phase structure of $N_f = 3$ QCD with massless or light degenerate quarks in §2.2. We emphasized that at $T = 0$, the low density hadronic phase and the high density quark phase might be continuously connected. On the other hand, there has to be a phase transition that separates the color-flavor locked phase from the

$T = \mu = 0$ hadronic phase. This is because of the presence of a gauge invariant $U(1)$ order parameter that distinguishes the two. In the case of $N_f = 3$ massless flavors the finite temperature phase transition is known to be first order. We expect the transition from the superconducting to the normal phase at $T \neq 0$ and large μ to be first order, too. This means that there is no tricritical point in figure 3c.

The phase diagram becomes more complicated if we take into account the effects of a finite strange quark mass (figure 3d). If $m_s^2/(4\mu) \sim \Delta$, there is a phase transition between the $N_f = 2+1$ phase with separate pairing in the *ud* and *ss* sectors and the CFL phase with pairing in both *ud* and *us* as well as *ds* sectors. Near this phase transition we may encounter phases with inhomogeneous BCS (LOFF) pairing [25]. Inside the CFL phase kaon condensation is a possibility.

The phase diagram shown in figure 3d should, at best, be considered an educated guess. Whether for realistic values of the quark masses there is an interlude of the 2SC phase along the $\mu \neq 0$ axis, instead of a direct transition between the CFL phase and nuclear matter, cannot be decided on the basis of currently available calculations. We know that there is at least one phase transition, because nuclear matter and the color-flavor locked phase are distinguished by a gauge invariant $U(1)_s$ order parameter. This, of course, is based on our belief that nuclear matter is stable with respect to strange quark matter or hyperonic matter. Current calculations have also not conclusively answered the question whether the transition along the $T \neq 0$ axis is a smooth crossover, as indicated in figure 3d and favored by some lattice calculations, or whether the transition is first order, as would be the case if m_s is sufficiently small. This is clearly an important question in connection with the existence of the tricritical point.

The challenge ahead of us is to find experimental observables, both in heavy ion collisions and the observation of neutron stars, that will allow us to determine the phase diagram of hot and dense matter.

References

[1] S C Frautschi, Asymptotic freedom and color superconductivity in dense quark matter, in: *Proc. Workshop on Hadronic Matter at Extreme Energy Density* edited by N Cabibbo (Erice, Italy, 1978)

[2] B C Barrois, *Nucl. Phys.* **B129**, 390 (1977)

[3] F Barrois, *Nonperturbative effects in dense quark matter*, Ph.D. thesis (Caltech UMI 79-04847-mc (microfiche))

[4] D Bailin and A Love, *Phys. Rep.* **107**, 325 (1984)

[5] N Evans, S D Hsu and M Schwetz, *Nucl. Phys.* **B551**, 275 (1999)

[6] T Schäfer and F Wilczek, *Phys. Lett.* **B450**, 325 (1999)

[7] W E Brown, J T Liu and H C Ren, *Phys. Rev.* **D62**, 054016 (2000)

[8] T Schäfer, *Phys. Rev.* **D62**, 094007 (2000)

[9] M Alford, K Rajagopal and F Wilczek, *Phys. Lett.* **B422**, 247 (1998)

[10] R Rapp, T Schäfer, E V Shuryak and M Velkovsky, *Phys. Rev. Lett.* **81**, 53 (1998)

[11] D T Son, *Phys. Rev.* **D59**, 094019 (1999)

[12] T Schäfer and F Wilczek, *Phys. Rev.* **D60**, 114033 (1999)

[13] R D Pisarski and D H Rischke, *Phys. Rev.* **D61**, 074017 (2000)

[14] D K Hong, V A Miransky, I A Shovkovy and L C Wijewardhana, *Phys. Rev.* **D61**, 056001 (2000)

[15] W E Brown, J T Liu and H C Ren, *Phys. Rev.* **D61**, 114012 (2000)

[16] Q Wang and D H Rischke, nucl-th/0110016
[17] T Schäfer, *Nucl. Phys.* **B575**, 269 (2000)
[18] N Evans, J Hormuzdiar, S D Hsu and M Schwetz, *Nucl. Phys.* **B581**, 391 (2000)
[19] M Alford, K Rajagopal and F Wilczek, *Nucl. Phys.* **B537**, 443 (1999)
[20] T Schäfer and F Wilczek, *Phys. Rev. Lett.* **82**, 3956 (1999)
[21] D V Deryagin, D Yu Grigoriev and V A Rubakov, *Int. J. Mod. Phys.* **A7**, 659 (1992)
[22] E Shuster and D T Son, *Nucl. Phys.* **B573**, 434 (2000)
[23] M Alford, J Berges and K Rajagopal, *Nucl. Phys.* **B558**, 219 (1999)
[24] T Schäfer and F Wilczek, *Phys. Rev.* **D60**, 074014 (1999)
[25] M G Alford, J Bowers and K Rajagopal, *Phys. Rev.* **D63**, 074016 (2001)
[26] T Schäfer, *Phys. Rev. Lett.* **85**, 5531 (2000)
[27] P F Bedaque and T Schäfer, hep-ph/0105150
[28] D B Kaplan and S Reddy, hep-ph/0107265
[29] R Casalbuoni and D Gatto, *Phys. Lett.* **B464**, 111 (1999)
[30] C Manuel and M H Tytgat, *Phys. Lett.* **B479**, 190 (2000)
[31] D K Hong, *Phys. Lett.* **B473**, 118 (2000)
[32] D K Hong, *Nucl. Phys.* **B582**, 451 (2000)
[33] S R Beane, P F Bedaque and M J Savage, *Phys. Lett.* **B483**, 131 (2000)
[34] T Schäfer, hep-ph/0109052
[35] D T Son and M Stephanov, *Phys. Rev.* **D61**, 074012 (2000); erratum: hep-ph/0004095
[36] J Berges and K Rajagopal, *Nucl. Phys.* **B538**, 215 (1999)
[37] M A Halasz, A D Jackson, R E Shrock, M A Stephanov and J J Verbaarschot, *Phys. Rev.* **D58**, 096007 (1998)
[38] M Stephanov, K Rajagopal and E V Shuryak, *Phys. Rev. Lett.* **81**, 4816 (1998)